

Supporting Information

Enhancement in Efficiency and Optoelectronic Quality of Perovskite Thin Films Annealed in MACl Vapor

Dhruba B. Khadka† Yasuhiro Shirai†, Masatoshi Yanagida† Takuya Masuda† and Kenjiro Miyano†

†Global Research Center for Environment and Energy based on Nanomaterials Science (GREEN), National Institute for Materials Science (NIMS), 1-1 Namiki, Tsukuba, Ibaraki 305-0044, Japan.

Corresponding Author:

* E-mail: SHIRAI.Yasuhiro@nims.go.jp

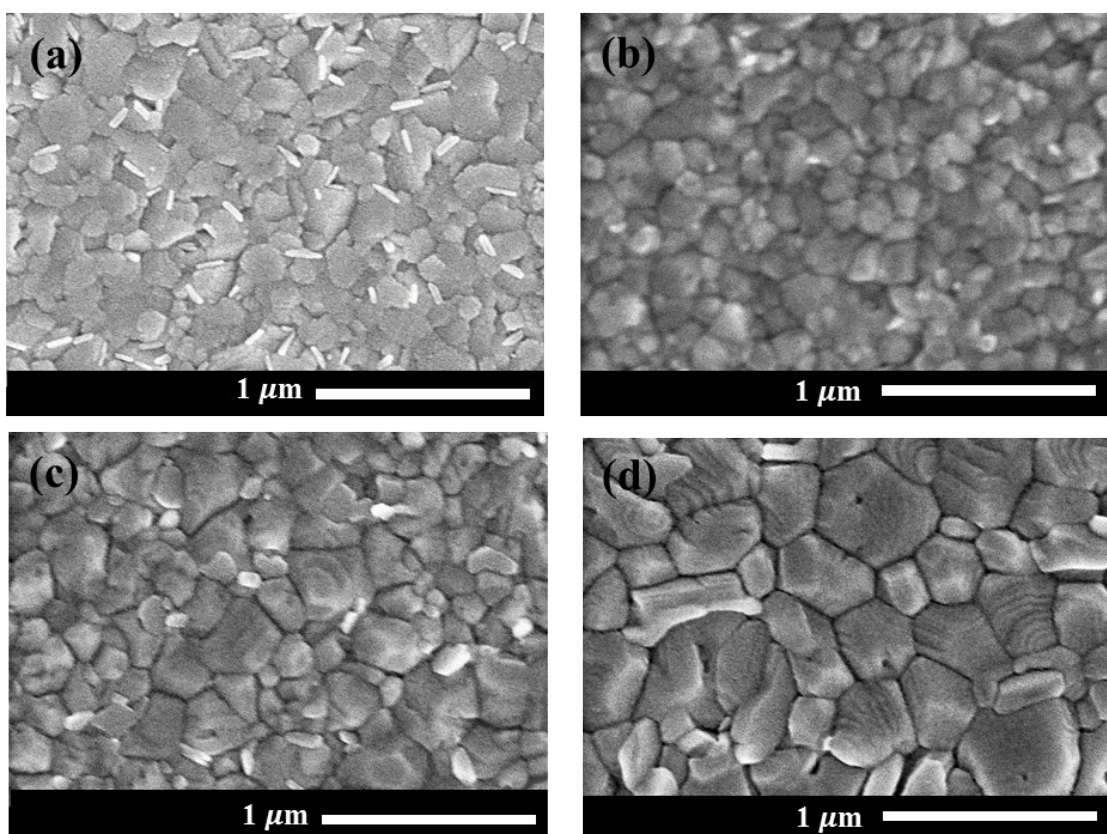
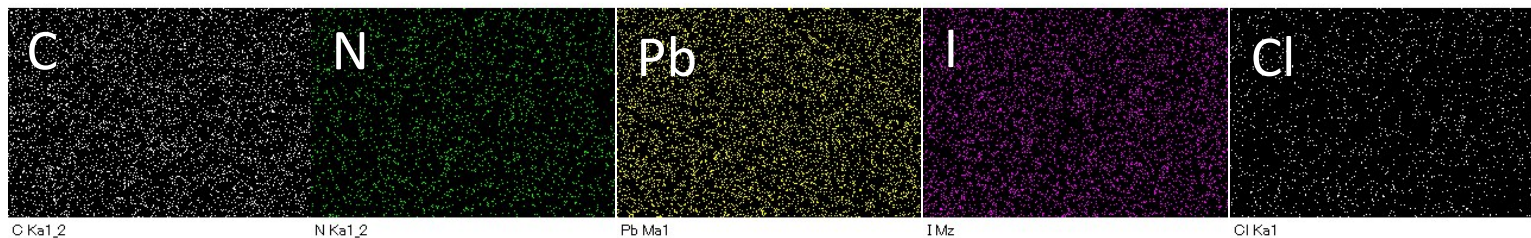
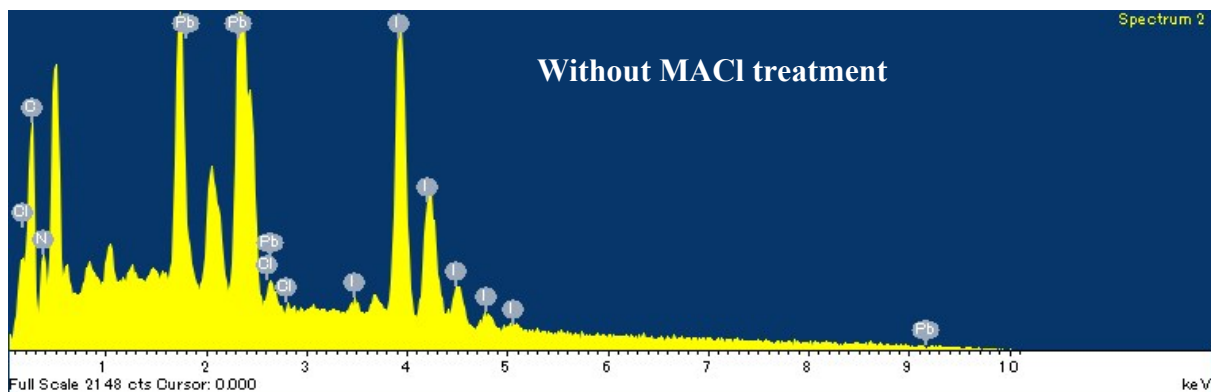


Figure S1. Surface images of samples (a) PbI_2 film, (b) as-deposited perovskite film, perovskite films (c) without MACl treatment, and (d) with MACl treatment.



Element	App	Intensity	Weight%	Weight%	Atomic%
	Conc.	Corn.		Sigma	
C K	0.17	1.256	6.57	0.22	37.48
N K	0.05	0.556	4.16	0.26	20.35
Cl K	0.00	1.054	0.16	0.10	0.30
I L	1.14	0.938	59.39	0.47	32.05
Pb M	0.55	0.899	29.72	0.44	9.82

Figure S2.

Elemental

composition distribution in a perovskite film without MAI treatment by EDS mapping.



Element	App	Intensity	Weight%	Weight%	Atomic%
	Conc.	Corn.		Sigma	
C K	0.17	1.256	6.57	0.22	37.48
N K	0.05	0.556	4.16	0.26	20.35
Cl K	0.00	1.054	0.17	0.10	0.32
I L	1.14	0.938	59.38	0.47	32.05
Pb M	0.55	0.899	29.72	0.44	9.82

Figure S3.
composition

Elemental
distribution

in a perovskite film with MACl treatment by EDS mapping.

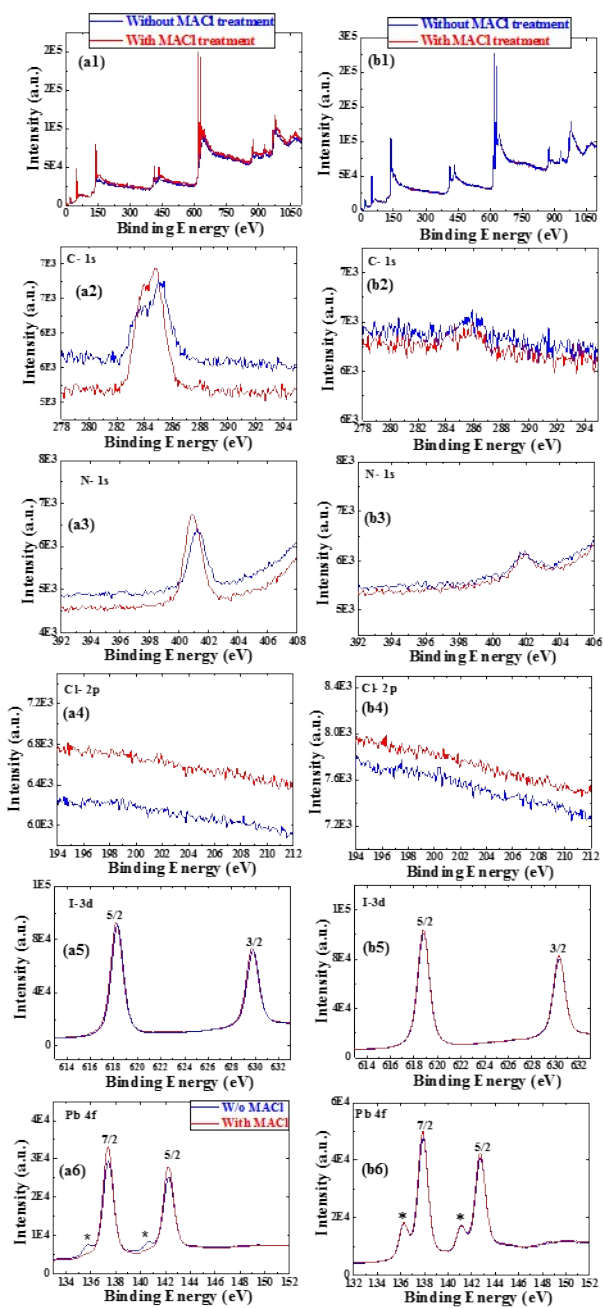


Figure S4. XPS spectra of perovskite thin films with and without MACl treatment. Left panels are data obtained from the surface of the films and right panels are those from the bulk after etching 80 nm deep.

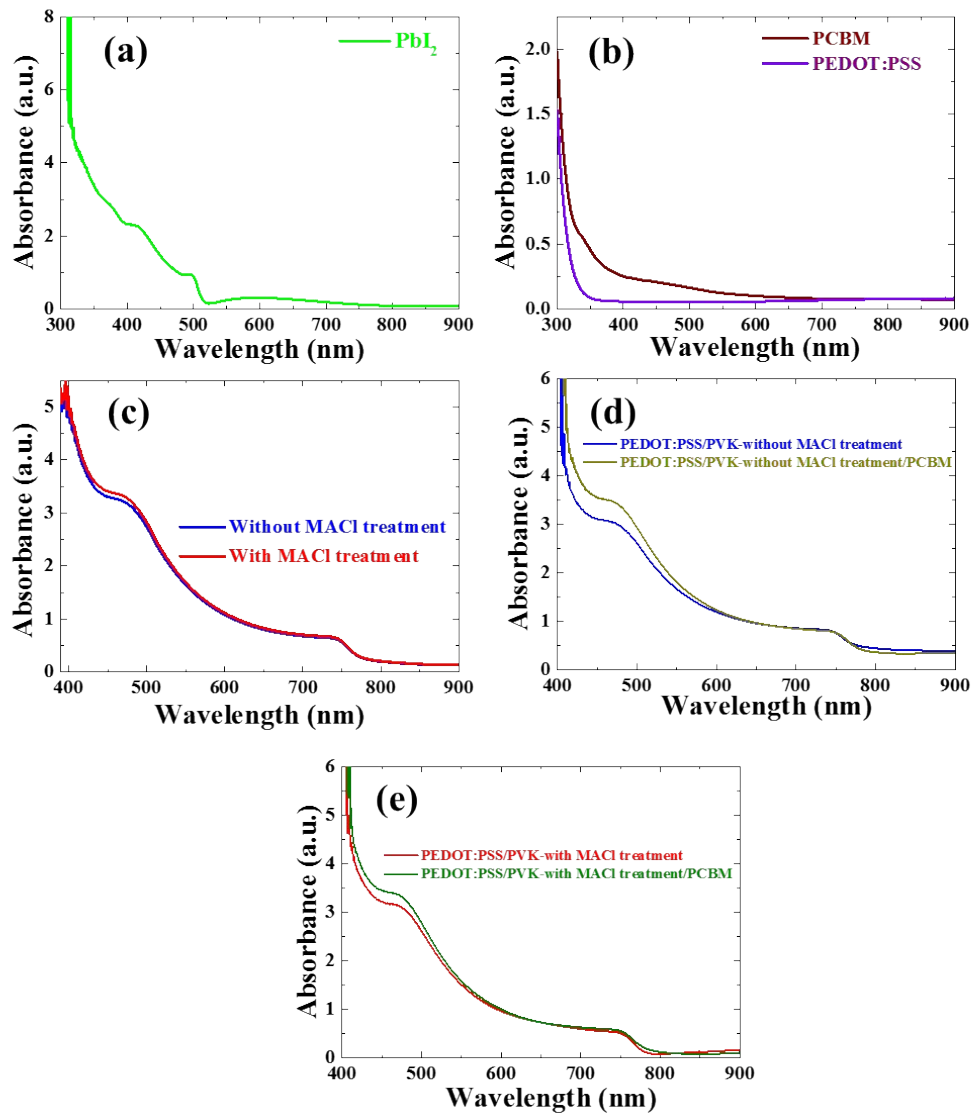


Figure S5. Absorption spectra of PbI₂ film (a), PEDOT: PSS (HTM) and PCBM (ETM) films (b), Glass/perovskite (PVK) (c), PEDOT:PSS/PVK and PEDOT:PSS/PVK/PCBM films without MACl treatment (d), and with treatment (e).

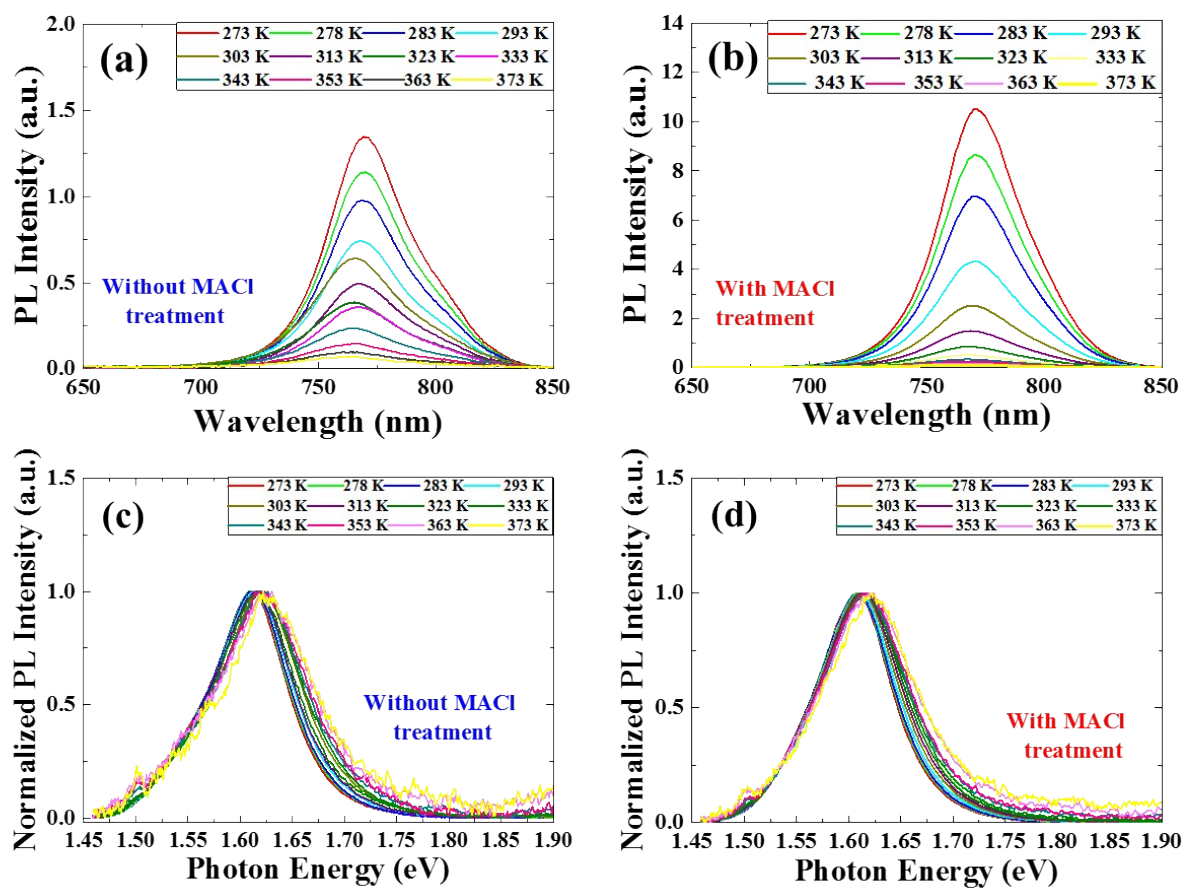


Figure S6. Temperature dependent PL spectra of perovskite films prepared with and without MACl treatment (a, b) in the range of 273 K- 373 K. Normalized PL spectra of respective films (c, d).

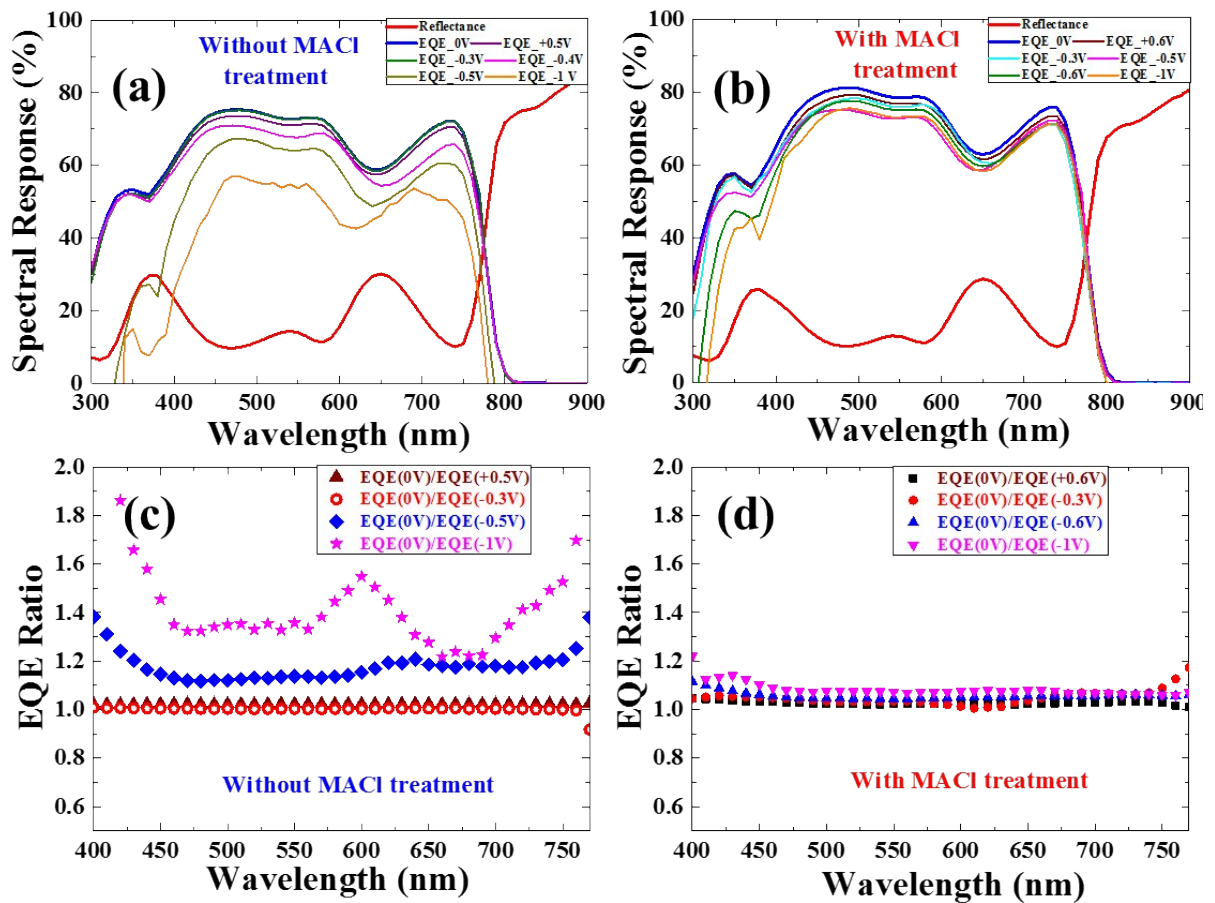


Figure S7. EQE response of respective devices measured under different bias voltage (a,b) and EQE ratio with respect to EQE at 0V bias.

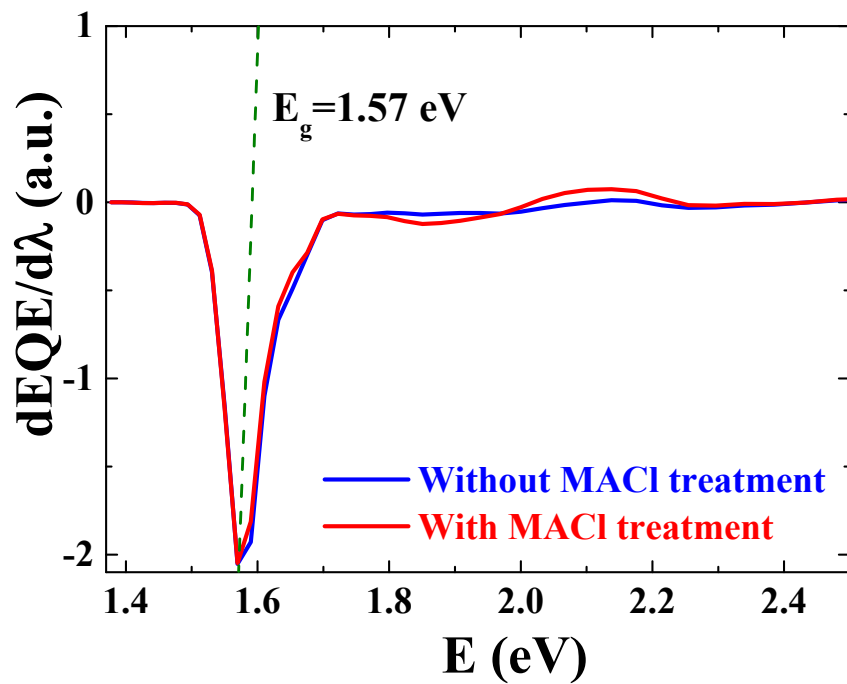


Figure S8. Estimation of band gap energy of perovskite thin films from the EQE spectra of respective devices with and without MACl treatment.

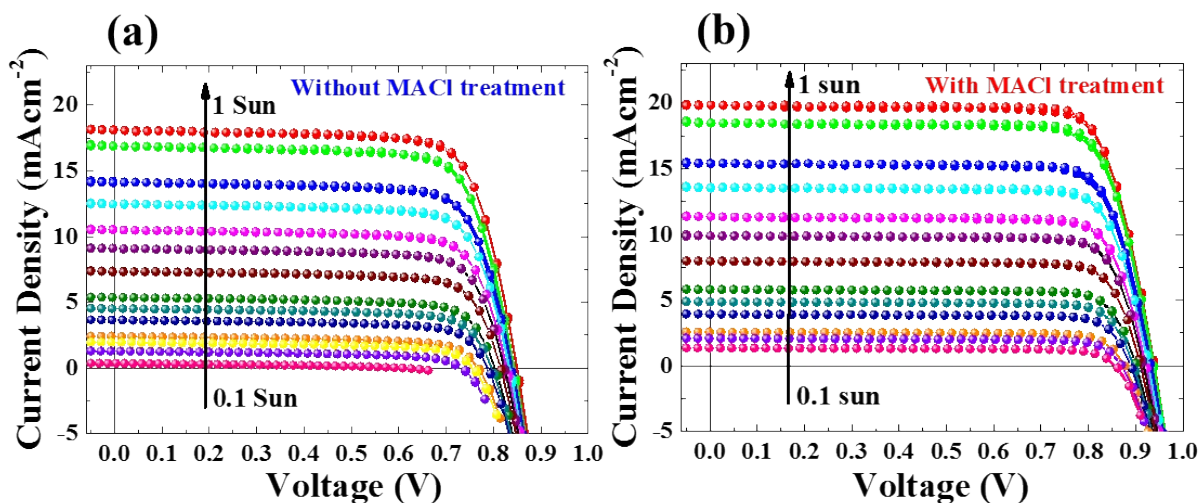


Figure S9. Current density–voltage (J-V) results of devices without (a) and with (b) MACl treatment measured under different light intensity.

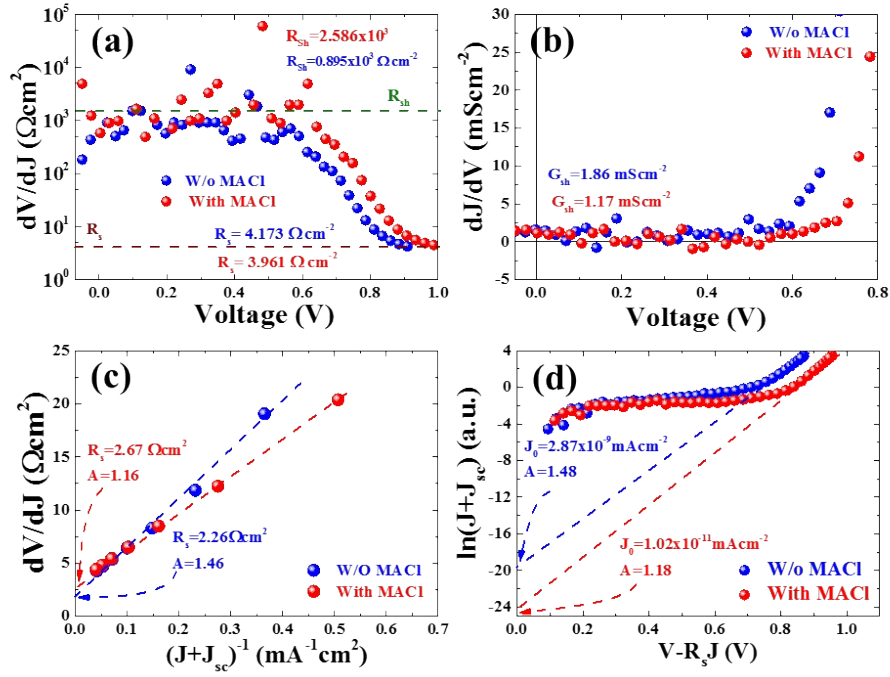


Figure S10. Analysis of J-V results of devices of respective types for the estimation of opto-electronic properties; series/shunt resistance (R_s , R_{sh}), shunt conductance (G_{sh}), diode ideality factor (A) and reverse saturation current (J_0). The calculation were carried out adopting earlier reports and close agreement to reported results.¹⁻³

Source Plots	Parameters	Devices	
		without MACI treatment	with MACI treatment
Fig.S10a	$R_{sh}(\Omega\text{cm}^2)$	8.95×10^2	2.58×10^3
	$R_s(\Omega\text{cm}^2)$	4.17	3.96
Fig.S10b	$G_{sh}(\text{mScm}^{-2})$	1.89	1.17
Fig.S10c	$R_s(\Omega\text{cm}^2)$	2.26	2.67
	A	1.46	1.16
Fig.S10d	$J_0(\text{mAcm}^{-2})$	2.87×10^{-9}	1.02×10^{-11}
	A	1.48	1.18
Fig. 5a	A	1.45	1.08

Table S1. Estimated opto-electronic properties of the devices with and without MAI treatment.

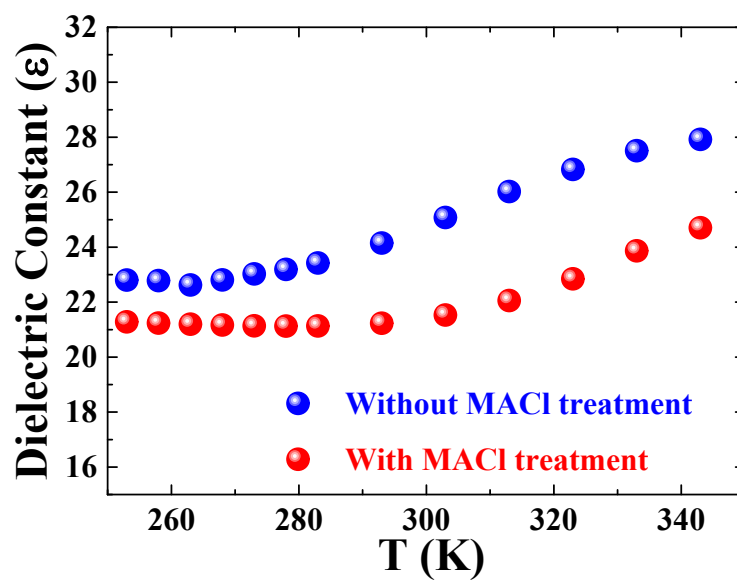


Figure S11. Plot of dielectric constant of perovskite films prepared with and without MAI treatment extracted from analysis of C-f spectra as depicted in Figure 9a,b.

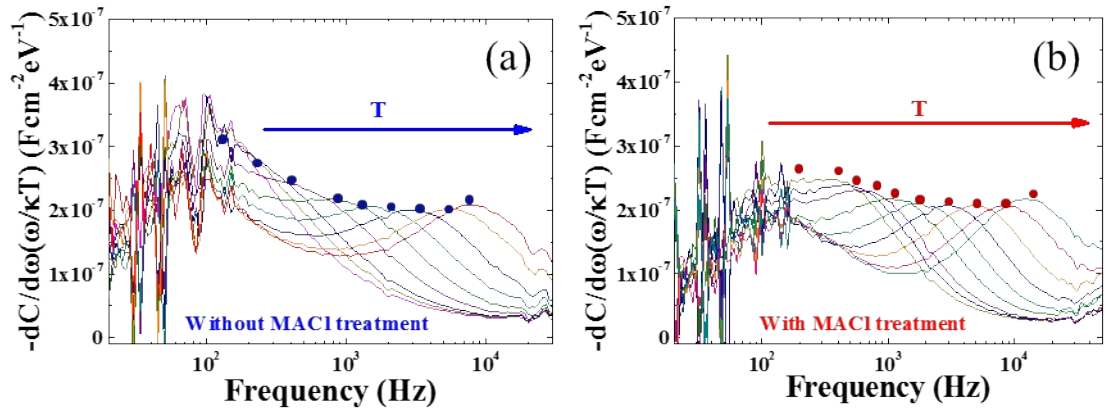


Figure S12. Plots of differentiation of C-f spectra (as shown in Figure 9a, b) for determination of inflection frequencies

Table S2. Summary of simulation parameters of perovskite solar cell devices for SCAPS simulation. The device layers were defined considering the earlier reports on similar kind of solar cell.⁴⁻⁷ (HTM: hole transport material, ETM: electron transport material, and IF: interface layer.)

Material /Properties	HTM	IF-2	Perovskite	IF-1	ETM
X(μm)	0.035	0.015	0.350	0.010	0.060
E_g (eV)	3.2	1.55	1.55	1.55	3.2
χ (eV)	2.45	3.9	3.9	3.9	4.0
ϵ_r	3	22	22	22	3
N_c (cm^{-3})	2.2×10^{18}				
N_v (cm^{-3})	1.8×10^{19}				
v_n (cm s^{-1})	1×10^7				
v_h (cm s^{-1})	1×10^7				

μ_n/μ_h (cm ² V ⁻¹ s ⁻¹)	$5 \times 10^{-4}/5 \times 10^{-4}$	2/2	4/4	1/1	$5 \times 10^{-4}/5 \times 10^{-4}$
N_d (cm ⁻³)	-	1×10^{14}	1×10^{14}	1×10^{14}	5×10^{18}
N_a (cm ⁻³)	1×10^{19}	1×10^{14}	1×10^{14}	1×10^{14}	-
N_t (cm ⁻³)	1×10^{16}	$1 \times 10^{14} - 1 \times 10^{20}$	$5 \times 10^{13} - 5 \times 10^{15}$	$1 \times 10^{14} - 1 \times 10^{20}$	1×10^{16}
CC of e/h (cm ²)	$5 \times 10^{-14}/5 \times 10^{-14}$	$5 \times 10^{-14}/5 \times 10^{-14}$	$2 \times 10^{-14}/2 \times 10^{-14}$	$5 \times 10^{-14}/5 \times 10^{-14}$	$5 \times 10^{-14}/5 \times 10^{-14}$
E_t (eV)/distribution	0.5/Gau	0.5/Gau	(0.2-0.5 /Gau	0.5/Gau	0.5/Gau
Interface; CC (cm ²)/ E_t (eV)/ N_t (cm ⁻³)	HTM/IF-2; $1 \times 10^{-14}/0.8/1 \times 10^{18}$			ETM/IF-1 $1 \times 10^{-14}/0.8/1 \times 10^{18}$	

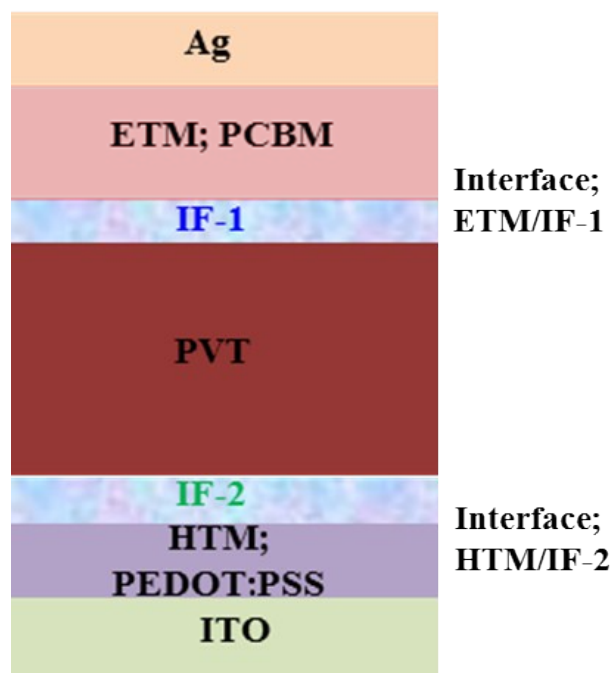


Figure S13. Schematic diagram of device layer defined for SCAPS simulation.

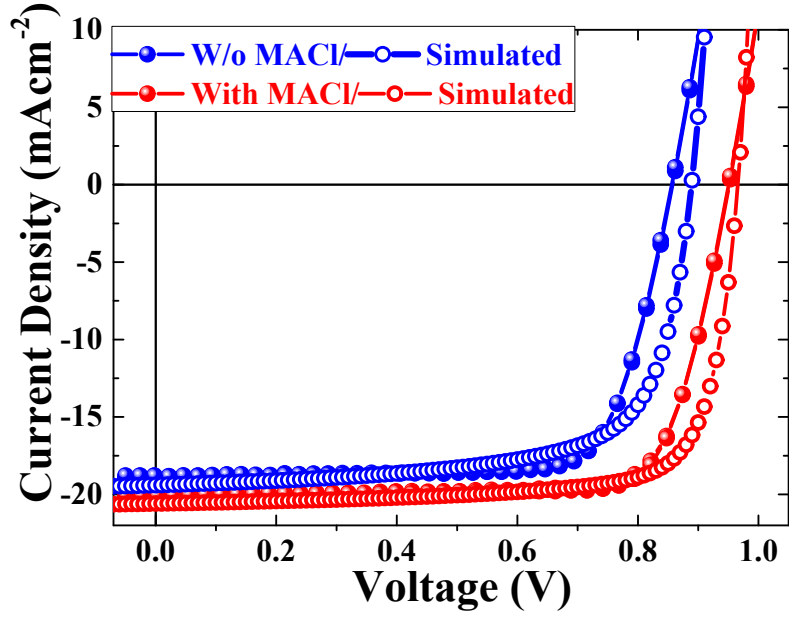


Figure S14. Current density–voltage (J-V) characteristics of devices fabricated with and without MACl treatment (Fig. 6a) and those from simulation. The simulated J-V results were obtained by device simulation using defect levels (E_t)~0.34 and 0.47 eV for MACl untreated device and ~0.24 and 0.35 eV for treated device, estimated from Arrhenius plot (Figure 9c). The bulk defect density was assumed to be $10^{16} \text{ cm}^{-3} \text{ eV}^{-1}$ for the former and slightly higher for the latter in accordance with the experimental result (Figure 9d). These values are slightly smaller than calculated from the experiment data but within the acceptable range. Other parameters are the same as summarized in Table S2.

Table S3. Summary of the device parameters obtained from experiment and simulation.

Device type/ Device parameter	Without MACl treatment		With MACl treatment	
	Experimental	Simulated	Experimental	Simulated
Voc(V)	0.86	0.89	0.95	0.96
Jsc(mAcm ⁻²)	18.80	19.42	20.06	20.59
FF (%)	77.08	70.83	79.15	77.08
η (%)	12.41	12.33	15.09	15.33

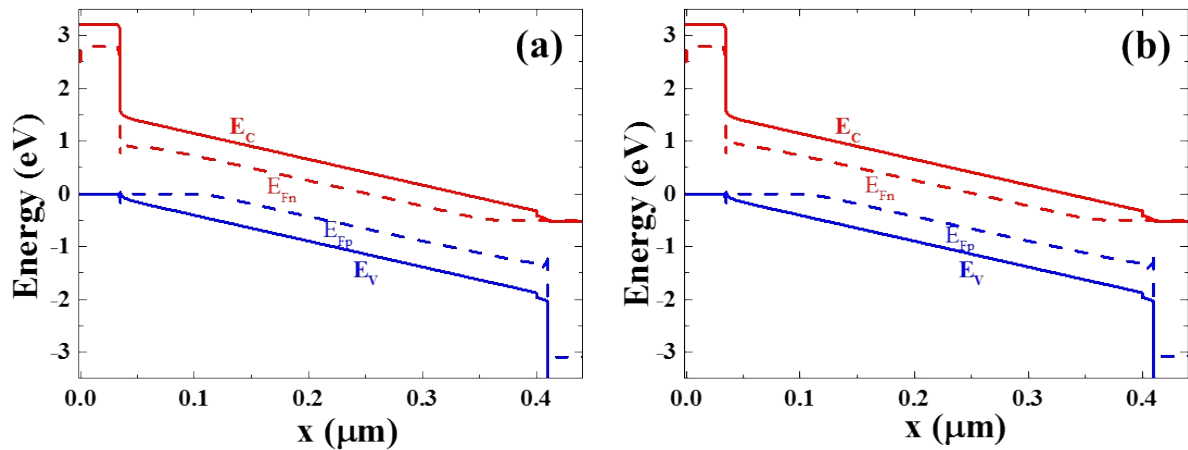


Figure S15. Simulated energy band (EB) diagram of respective devices [from parameters defined for devices (a) without MACI treatment and (b) with MACI treatment] from SCAPS simulation. The parameters corresponding to simulated J-V results as presented in Figure S14 are used. No clear difference between the two devices is observed.

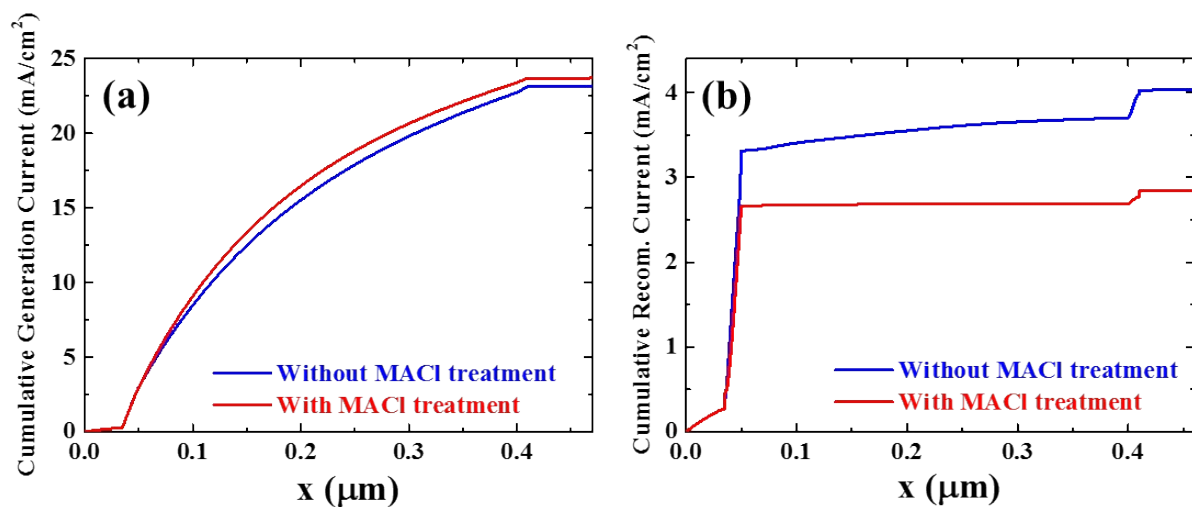


Figure S16. Simulated results of cumulative generation and recombination current of respective devices with defined parameters corresponding to simulated J-V data (Figure S14). The generation current is slightly higher whereas the cumulative recombination current is quite lower for the MACI treated device. The lower recombination current at interface region (Figure b) could be related to improvement in interface layer quality which supports our experimental results.

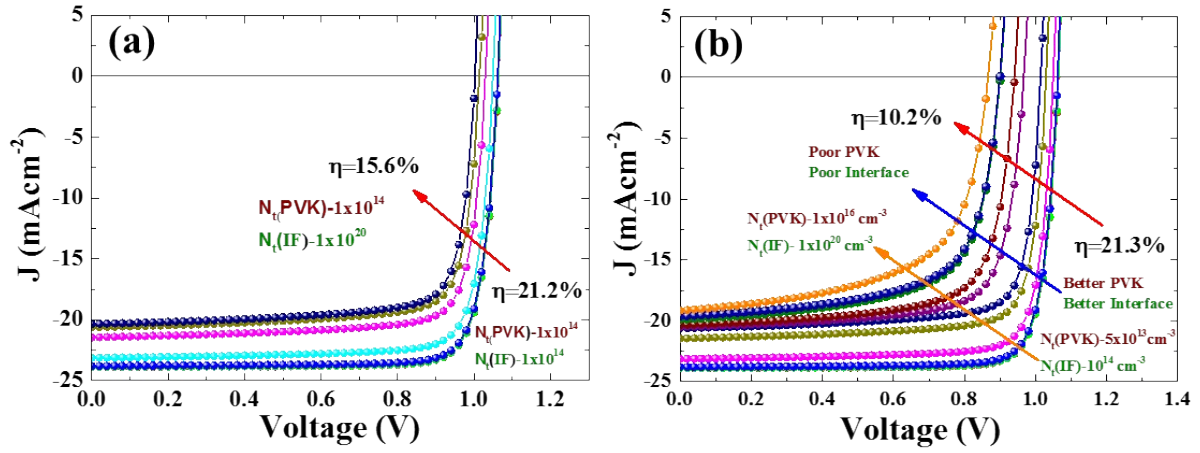


Figure S17. Impact on J-V curves of the defect density (N_t) at interface (IF) defect layer (a) and of the defect density in perovskite layer (PVK) and interface (b). Other parameters kept constant are taken from Table S2. Plot (a) shows effect of interface defect density (accounting interface layer quality) on J-V curves (device performances) indicating larger impact on J_{SC} . And the plot (b) depicts impact of quality of interface and perovskite bulk by varying defect density which indicates strong impacts on device performance with severe effect on all device parameters (J_{SC} , V_{OC} , FF). These results consolidate that our fabrication approach improves the quality of bulk perovskite as well as interface layer, supporting hypothesis.

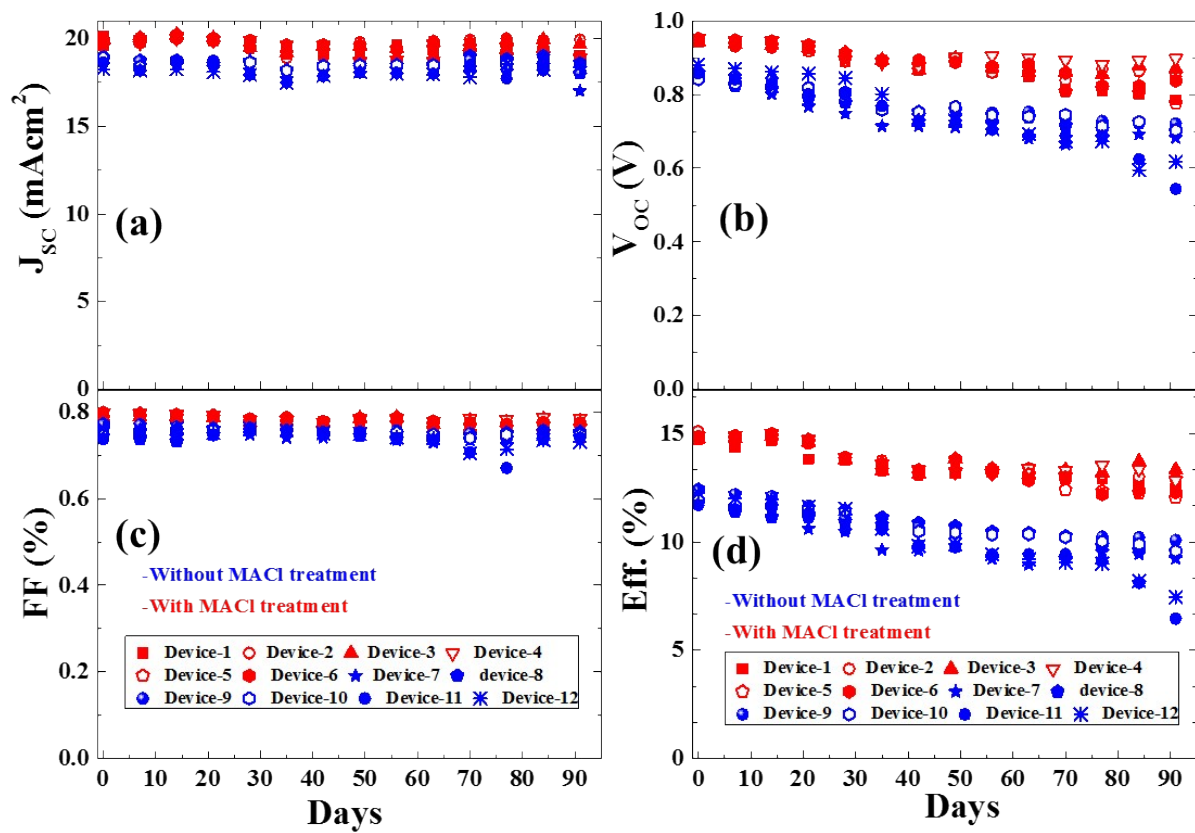


Figure S18. Stability data (solar cell parameter J_{sc} , V_{oc} , FF and Eff.) of encapsulated devices stored under ambient conditions for 3 months.

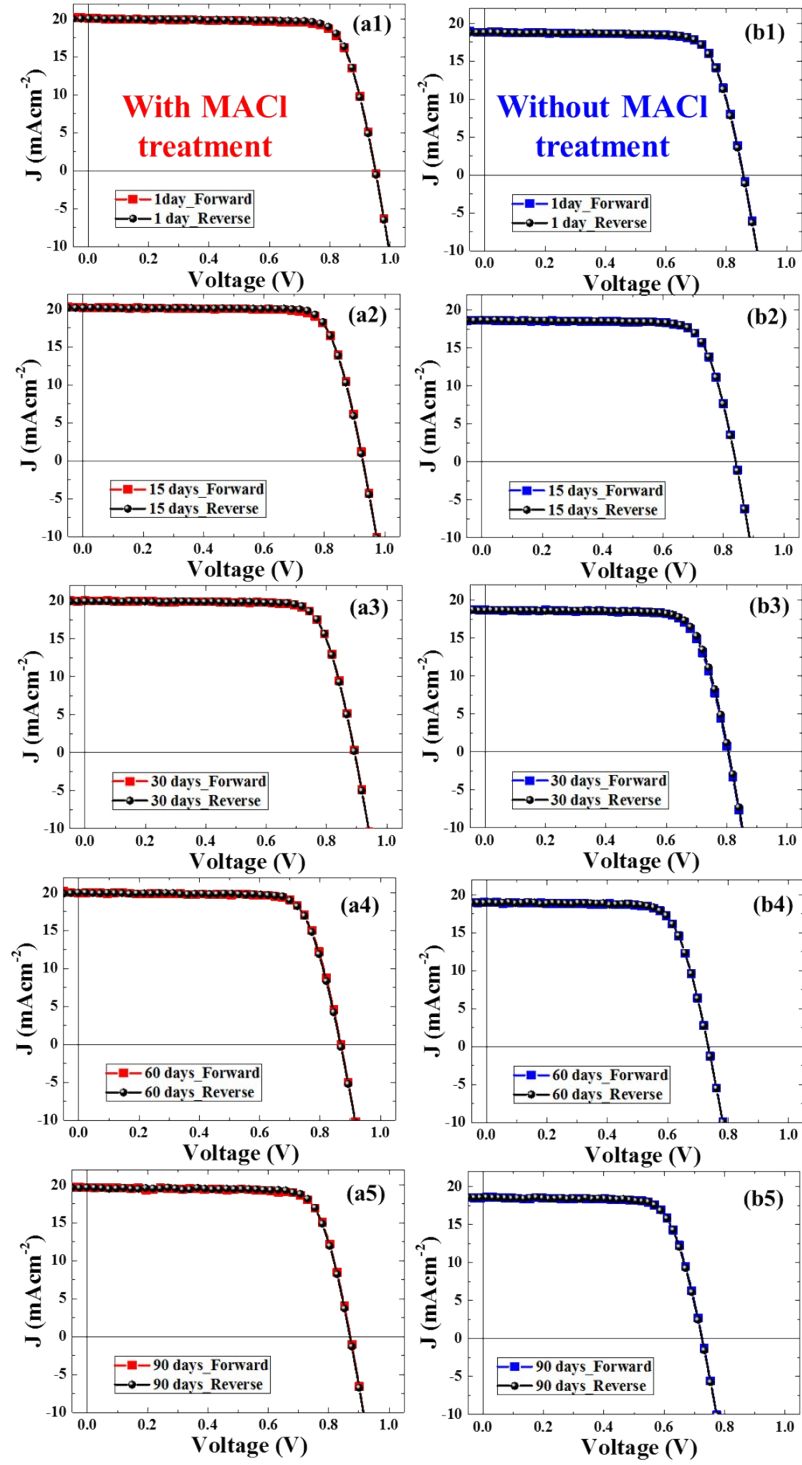


Figure S19. Change in J-V characteristics of devices over a period of 3 months.

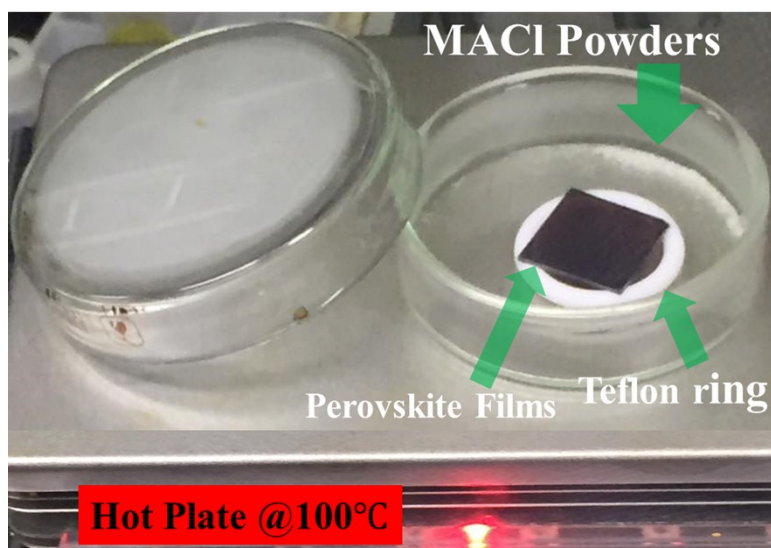


Figure S20. Experimental set up for the MACl treatment (petri dish walls have pale white appearance due to deposition of MACl vapors during the treatment). The temperature difference between the sample and the hotplate was less than 5°C with the experimental setup shown here.

References

1. S. S. Hegedus and W. N. Shafarman, *Progress in Photovoltaics: Research and Applications*, 2004, **12**, 155-176.
2. J. J. Shi, J. Dong, S. T. Lv, Y. Z. Xu, L. F. Zhu, J. Y. Xiao, X. Xu, H. J. Wu, D. M. Li, Y. H. Luo and Q. B. Meng, *Appl. Phys. Lett.*, 2014, **104**, 063901.
3. K. Miyano, M. Yanagida, N. Tripathi and Y. Shirai, *Appl. Phys. Lett.*, 2015, **106**, 093903.
4. J. Pettersson, M. Edoff and C. Platzer-Björkman, *J. Appl. Phys.*, 2012, **111**, 014509.
5. F. Liu, J. Zhu, J. F. Wei, Y. Li, M. Lv, S. F. Yang, B. Zhang, J. X. Yao and S. Y. Dai, *Appl. Phys. Lett.*, 2014, **104**.
6. T. Minemoto and M. Murata, *J. Appl. Phys.*, 2014, **116**, 054505.
7. K. Miyano, N. Tripathi, M. Yanagida and Y. Shirai, *Acc. Chem. Res.*, 2016, **49**, 303-310.